Microbiological Research **162** (2007) 355–368

Available online at www.sciencedirect.com
ScienceDirect

Microbiological Research
www.elsevier.de/micres

Biodegradation of corrosion inhibitors and their influence on petroleum product pipeline

Aruliah Rajasekar, Sundaram Maruthamuthu, Narayanan Palaniswamy*, Annamalai Rajendran

Biocorrosion, Corrosion Protection Division, Central Electrochemical Research Institute, Karaikudi–630 006, India

Accepted 15 February 2006

KEYWORDS
Diesel pipeline;
Corrosion inhibitors;
Rotating cage methods;
Biodegradation;
Microbiologically influenced corrosion

Summary

The present study enlightens the role of *Bacillus cereus* ACE4 on biodegradation of commercial corrosion inhibitors (CCI) and the corrosion process on API 5LX steel. *Bacillus cereus* ACE4, a dominant facultative aerobic species was identified by 16S rDNA sequence analysis, which was isolated from the corrosion products of refined diesel-transporting pipeline in North West India. The effect of CCI on the growth of bacterium and its corrosion inhibition efficiency were investigated. Corrosion inhibition efficiency was studied by rotating cage test and the nature of biodegradation of corrosion inhibitors was also analyzed. This isolate has the capacity to degrade the aromatic and aliphatic hydrocarbon present in the corrosion inhibitors. The degraded products of corrosion inhibitors and bacterial activity determine the electrochemical behavior of API 5LX steel.

Introduction

Generally the major bacteria involved in the microbially influenced corrosion are anaerobic sulfate reducing bacteria (SRB) (Hamilton, 1985; Voordouw et al., 1994; Graves and Sullivan, 1996; Pope and Pope, 1998; Jana et al., 1999), whose participation in corrosion was evidenced decades ago (Von Wolzogen Kuhr and Vander Klugt Water, 1934). However, aerobic bacteria and fungi participate in the corrosion process (Shennan, 1988; Videla and Characklis, 1992; Bento and Gaylarde, 2001). The microorganisms influence the corrosion by altering the chemistry at the interface between the metal and the bulk fluid (Jones and Amy, 2002; Little and Ray, 2002). SRB have been repeatedly detected in oil- and gas-producing facilities, as well as in transportation and storage facilities and are most likely the cause for the biocorrosion, souring and biofouling problems that often arise at these

*Corresponding author. Tel.: +91 4565 227550; fax: +91 4565 227779.
E-mail address: swamy23@rediffmail.com (N. Palaniswamy).

0944-5013/$ - see front matter © 2006 Elsevier GmbH. All rights reserved.
doi:10.1016/j.micres.2006.02.002

sites (Hamilton, 1985; Burger, 1998). The injection of sulfate-containing seawater into the reservoirs during the secondary recovery of oil favors the proliferation of the bacteria. Therefore, most of the research on microbially influenced corrosion has focused on SRB. However, recent studies suggest that SRB need not be present in abundance in the microbial communities responsible for microbially influenced corrosion (Zhu et al., 2003; Jan-Roblero et al., 2004). CECRI, India also recently noticed the absence of SRB in refined diesel (Maruthamuthu et al., 2005) and naphtha-transporting pipelines (Rajasekar et al., 2005). Microbial corrosion studies involving the use of natural individual species without SRB obtained from industrial systems are scarce (Muthukumar et al., 2003; Bento et al., 2005). However, such studies would better address the actual problem and increase the understanding of the microbial species involved in microbial corrosion and their interactions with metal surfaces. It will be useful for the development of new approaches for the detection, monitoring and control of microbial corrosion in industrial facilities.

Organic film-forming inhibitors used in the oil and gas industry are generally of the cationic/anionic type and include imidazolines, primary amines, diamines, amino-amines, oxyalkylated amines, fatty acids, dimmer, trimer acids, naphthaneic acid, phosphate esters and dodecyl benzene sulfonic acids. Their mechanism of action is to form a persistent monolayer film adsorbed at the metal/solution interface. Thus, the alteration of the molecule of the inhibitor caused by microbial degradation during their use, which can affect their specific performance on corrosion inhibition (Videla et al., 2000). Microbial degradation of simple heterocyclic inhibitor of the type morpholine (C_4H_9NO) has recently been reported (Poupin et al., 1998). The degradation involved an enzymatic attack at the C–N position, followed by ring cleavage to produce glycolic acid (Poupin et al., 1998). Romero Dominguez et al. (1998) reported the loss in efficiency of organic corrosion inhibitors in the presence of *Pseudomonas fluorescence* isolated from injection water system used in offsore oil production. Recently Maruthamuthu et al. (2005) has noticed the degradation of corrosion inhibitor and its effect on the corrosion process in a 1400 km petroleum product-transporting pipeline at Northwest, India. In petroleum product pipelines, it would be better to know if the corrosion inhibitor is acting as a nutrient source or as biocide, or indeed, of what its effect at all. In the present study, a laboratory experiment was designed to evaluate the degradation of corrosion inhibitor by employing dominating individual species *Bacillus cereus* ACE4, and its role on corrosion process in petroleum products.

Experimental

Background information of the study

A cross-country pipeline in North India transports petroleum products such as kerosene, petrol and diesel. This pipeline has intermittent petroleum product delivery cum pressure-booting stations at different locations. Severe corrosion and microfouling problems have been faced in the pipeline even though corrosion inhibitor was added. Within 30 days, about 200–400 kg of muck (corrosion product) was received from a 200 km stretch of the pipeline (Maruthamuthu et al., 2005). The corrosion product was pushed out of the pipeline by pigs (Cylindrical device that moves with the flow of oil and cleans the pipeline interior) while cleaning the pipeline. The corrosion product samples were collected in sterile containers for microbial enumeration and identification.

Bacterial identification in corrosion product

By using sterilized conical flasks, samples of corrosion products were collected from the diesel-transporting pipeline. These samples were transported using icebox from sites to Central Electrochemical Research Institute (CECRI) – mobile microbiological lab. The collected samples were serially diluted (10-fold) using 9 ml of sterile distilled water-blanks and the samples were plated by pour plate technique. The nutrient agar medium was used to enumerate heterotrophic bacteria. The collected samples were serially diluted up to 10^{-6} dilution. One millilitre (1 ml) of each sample was poured into sterile petridishes. The prepared sterile nutrient agar medium was poured into sterile petridishes. The plates were gently swirled so that the medium might be distributed evenly in the plate. Plates in triplicate were prepared for each dilution. The plates were inverted and incubated at room temperature for 24 h. After 24 h, the colonies were counted. Morphologically dissimilar colonies were selected randomly from all plates and isolated colonies were purified using appropriate medium by streaking methods. The pure cultures were maintained in slants for further analysis. The isolated bacterial cultures were identified by their morphological and biochemical characteristics at CECRI microbiological lab,

karaikudi. The isolated bacterial cultures were identified up to genus level by their morphological and biochemical characterization viz. gram staining, motility, indole, methyl red, voges-proskauer test, citrate test, H_2S test, carbohydrate fermentation test, catalase test, oxidase test, starch, gelatin, lipid hydrolysis, etc (Holt et al., 1994). Ten genera were identified in the corrosion product. The following genera were identified by biochemical test: *Bacillus* sp., *Micrococcus* sp., *Vibrio* sp., *Pseudomonas* sp., *Thiobacillus* sp., *Ochrobium* sp., *Xanthobacter* sp., *Gallionella* sp., *Legionella* sp. and *Acinetobacter* sp. The dominating genus *Bacillus* sp. (it has also been confirmed by Institute of Microbial Technology, Chandigarh by employing bio-chemical analysis) has been selected for further study, which was about 50% in pumping station II. Besides, the dominating genus was identified by16S rDNA gene analysis as *Bacillus cereus* ACE4, which was selected for further biodegradation and corrosion studies.

Amplification, cloning and sequencing of 16S rDNA gene

Genomic DNA was extracted according to Ausubel et al. (1988). Amplification of gene encoding for small subunit ribosomal RNA was carried out using eubacterial 16S rDNA primers (forward primer 5′AGAGTTTGATCCTGGCTCAG 3′ (*E. coli* positions 8–27) and reverse primer 5′ACGGCTACCTTGT TACGACTT3′ (*E. coli* positions 1494–1513) (Weisburg et al., 1991). Polymerase chain reaction (PCR) was performed with a 50-μl reaction mixture containing 2 μl (10 ng) of DNA as the template, each primer at a concentration of 0.5 μM, 1.5 mM $MgCl_2$ and each deoxynucleoside triphosphate at a concentration of 50 μM, 1 μl of *Taq* polymerase and buffer as recommended by the manufacturer (MBI Fermentas). PCR was carried out with a Mastercycler Personal (eppendorf, Germany) with the following program: initial denaturation at 95 °C for 1 min; 40 cycles of denaturation (1 min at 95 °C), annealing (1 min at 55 °C) and extension (2 min at 72 °C); followed by a final extension at 72 °C for 5 min. The amplified product was purified using GFX™ PCR DNA and Gel Band Purification kit (Amersham Biosciences) and in pTZ57R/T vector according to the manufacturer's instruction (InsT/Aclone™ PCR Product Cloning Kit, MBI Fermentas) and the transformants were selected on Luria bertana (LB) medium containing ampicillin (100 μg/ml) and X-gal (80 μg/ml). Sequencing reaction was carried out using ABI PRISM 310 Genetic Analyzer (PE Applied Biosystems). For sequencing reaction Big Dye Ready Reaction DyeDeoxy Terminator Cycle Sequencing kit (Perkin–Elmer) was employed. The obtained partial 16S rDNA sequence was then submitted to a BLAST (Altschul et al., 1990) search to obtain the best matching sequences. The nucleotide sequence data have been deposited in GenBank.

Biodegradation of corrosion inhibitors and their characterization

In the present study, commercially available inhibitors used in petroleum-transporting pipeline were evaluated to find out the nature of degradation, which was used in petroleum pipeline. The inhibitor I is dodecyl-carboxylic acid-based and inhibitor II is amine-based carboxylic acid compounds.

The medium used for detecting the corrosion inhibitor degrading process by ACE4 was Bushnell–-Hass broth (magnesium sulfate—0.20 gm/l; calcium chloride—0.02 gm/l; monopotassium phosphate—1 gm/l; di-potassium phosphate—1 gm/l; ammonium nitrate—1 gm/l; ferric chloride—0.05 gm/l, Hi-Media, Mumbai) and Bushnell–Hass agar. Three sets of Erlenmeyer flasks were used for the inhibitor degradation studies using the selected bacterial strains. Two sets of Erlenmeyer flasks containing 100 ml of the BH broth and 400 ppm of corrosion inhibitors I and II each with ACE4 having an optical density of 0.045 at 600 nm (initial load was about 2.1×10^9) were inoculated. An uninoculated control flask was incubated parallelly to monitor abiotic losses of the corrosion inhibitors' substrate. The flasks were incubated at 30 °C for 30 days in an orbital shaker (150 rpm). Total viable counts (TVC) for ACE4 cells were performed after incubation of inocula at different time periods (3, 5, 10, 20, 25 and 30 days). Enumeration of *B. cereus* ACE4 was carried out using the standard plating method and the colonies were counted after 48 h of incubation at 30 °C.

At the end of the 30 days of incubation period, the residual corrosion inhibitors I and II for each system of the entire flask were extracted with an equal volume of dichloromethane. Evaporation of solvent was carried out in a hot water bath at 40 °C. The 1 μl of the resultant solution was analyzed by Fourier-transform infrared spectroscopy (FTIR) and H^1 Nuclear magnetic resonance spectroscopy (NMR). FTIR spectrum (Nicolet Nexus 470) was taken in the mid-IR region of 400–4000 cm^{-1} with 16-scan speed. The samples were mixed with spectroscopically pure KBr in the ratio of 1:100 and the pellets were fixed in the sample holder, and then the analysis was carried out. Infrared peaks

localized at 2960 and 2925 cm^{-1} were used to calculate the CH_2/CH_3 ratio (absorbance) and functional group of both aliphatic and aromatic components present in corrosion inhibitors. H^1 NMR (Bruker, 300 m Hz) analysis was used to detect the protons of the nuclei in the diesel compound. The sample of diesel was dissolved using deutrated chloroform solvent. Tetra methyl silane (TMS) was used as a reference standard.

The corrosion inhibitors I and II were characterized to find out the quantitative degradation by employing high performance liquid chromatography (HPLC) and gas chromatography-mass spectroscopy (GC-MS), respectively. Since inhibitor I could not be characterized by GC-MS because of the nature of the product, HPLC has been employed for the quantitative degradation. The 1 μl of the resultant corrosion inhibitor solution was analyzed by Thermo Finnigan gas chromatography/mass spectrometry (Trace MS equipped with an RTX-5 capillary column (30 m long × 0.25 mm internal diameter) and high purity nitrogen as carrier gas. The oven was programmed between 80 and 250 °C with a heating temperature of 10 °C/min. The GC retention data of the inhibitor correspond to the structural assignations carried out after Wiely library search with a database and by mass spectra interpretation. The HPLC solvent delivery system that consisted of analytical–shim-pack CLC-OCTA DECYL SILANE (ODS-C18, 4.6 mm ID, 25 cm) and UV-spectrophotometric (240 nm) were from SHIMADZU, Japan. The volume of sample injection is a loop full of 20 μl with the flow rate 1 ml/min. The mobile phase is methanol.

Inhibitor efficiency test

Rotating cage test

Corrosion inhibition efficiency was studied by rotating cage test (ASTM G170, Papavinasam et al., 2000). API 5LX grade steel (C-0.29 max, S-0.05 max, P-0.04 max, Mn-1.25 max.) coupons of size 2.5 × 2.5 cm were mechanically polished to mirror finish and then degreased using trichloro ethylene. Four coupons supported by polytetro fluro ethylene (PTFE) disks were mounted at 55 mm apart on the rotatory rod. Holes were drilled in the top and bottom PTFE plates of the cage in order to increase the turbulence on the inside surface of the coupon. The rotatory rod runs at 200 rpm, which corresponds to a linear velocity of 0.53 m/s. In the present study the following systems were used: 500 ml of diesel with 2% water containing 120 ppm chloride as a control system I; 500 ml of diesel with 2% water containing 120 ppm chloride and 2 ml of inoculum about 10^8 CFU/ml as a control system II; 500 ml of diesel with 2% water containing 120 ppm chloride and 10 ppm of corrosion inhibitors I and II each and marked as systems III and IV; while 500 ml diesel with 2% of water containing 120 ppm chloride, 10 ppm of corrosion inhibitor I and II each with 1% BH broth for bacterial growth and inoculated with 2 ml of inoculum about 10^8 CFU/ml as the experimental systems V and VI, respectively. Since bacteria need inorganic nutrients, BH broth has been added in the presence of bacterial system. After 7 days, the coupons were removed and washed in Clark's Solution for 1 min to remove the corrosion products, rinsed with sterile distilled water, and then dried. Final weights of the six coupons in each system were taken and the average corrosion rates were also calculated and standard deviations are also presented. The inhibition efficiency (IE) was calculated as follows:

$$\text{Inhibition efficiency (IE\%)} = \frac{W - W_{inh}}{W} \times 100,$$

where W_{inh} and W are the values of the weight-loss of steel after immersion in solutions with and without inhibitor, respectively.

Electrochemical methods for the evaluation of inhibitors

After the weight-loss experiments (rotating test), electrochemical tests were carried out in a special cell containing aqueous medium collected from the rotating cage (Schiapparelli and Meybaum, 1980). API 5LX steel coupon of size 1 cm^2 (0.155 $inch^2$) as working electrode, and a standard calomel electrode (SCE) and a platinum wire as counter electrode were employed for impedance and polarization studies. An EG & G electrochemical impedance analyzer (Model M6310 with software M398) was used for AC impedance measurements. After attainment of a steady-state potential, an AC signal of 10 mV amplitude was applied and impedance values were measured for frequencies ranging from 0.01 to 100 Hz. The values of R_{ct} were obtained from the Nyquist plots. After finishing the impedance study, the same coupons were used for polarization for avoiding the film disturbance in the oxide film in the presence of bacteria. The tafel polarization curves were obtained by scanning the potential from the open circuit potential toward 200 mV anodically and cathodically. The scan rate was 120 mV/min. Polarization measurements were carried out potentiodynamically using model PGP201, employing potentiostat with volta master-1-software.

Surface analysis study

To verify the adsorption of inhibitor on the metal surface in rotating cage test after 10 days, the film formed on the metal surface was carefully removed and dried, mixed thoroughly with potassium bromide (KBr) and made as pellets. These pellets are subjected to FTIR spectra (Perkin–Elmer, Nicolet Nexus −470) to find out the protective film formed on the surface of the metal coupons.

Results and discussion

In oil pipelines, water can also stratify at the bottom of line if the velocity is less than that required to entrain water and sweep it through the pipeline system. Liquids (hydrocarbon) stratify along the bottom of the pipe, with water forming a separate layer beneath the liquids where hydrocarbon degradation occurs at the interface easily by microbes. Hence, the role of bacteria on degradation and corrosion is an important area in petroleum product pipelines. The involvement of bacterial species on corrosion inhibitor degradation and corrosion has been studied by various investigators (Freiter, 1992; Prasad, 1998; Videla et al., 2000; Maruthamuthu et al., 2005). This is the first study that enlightens the role of individual species of *Bacillus cereus* ACE4 on biodegradation of corrosion inhibitor in petroleum products and its influence on corrosion process in tropical countries.

Identification of bacterial isolates

The diesel hydrocarbon biodegradative strain ACE4 was isolated from the corrosion product of diesel-transporting pipeline, North India. The preliminary identification of ACE4 by biochemical test indicated that the isolate belongs to the genus *Bacillus* sp. Phenotypic profile of strain ACE4 is shown in Table 1. Amplification of gene encoding for small subunit ribosomal RNA of ACE 4 was carried out using eubacterial 16S rDNA primers. The 16S rDNA amplicons derived from ACE4 was cloned in pTZ57R/T vector. The recombinant plasmid (pACE4, harboring 16S rDNA insert) was partially sequenced. The sequence obtained was matched with the previously published sequences available in NCBI using BLAST. Sequence alignment and comparison revealed more than 99% similarity with *Bacillus cereus*. The nucleotide sequence data have been deposited in GenBank under the sequence number AY912105.

Biodegradation analysis

Enumeration of bacteria

The total viable count of bacteria in the presence and in the absence of corrosion inhibitors I and II during degradation is presented in Fig. 1. The count is ranging between 10^4 and 10^7 in the presence of inhibitor I, while in the presence of inhibitor II, the count is rangingbetween 10^6 and 10^9. In the absence of corrosion inhibitor, the ACE4 count decreased ranging between 1.1×10^1 and 2.31×10^2 was noticed, although initial load (2.1×10^9) was same in all the systems. The proliferation of bacteria is higher in the presence

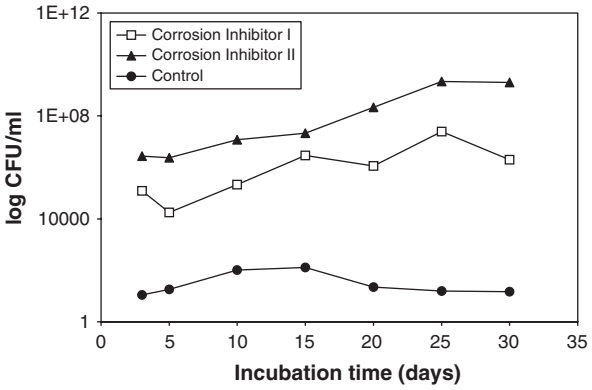

Figure 1. Growth of *Bacillus cereus* ACE4 in BH liquid medium in the presence and absence of corrosion inhibitors I and II.

Table 1. Biochemical characterization of strain ACE4

Positive test	Negative test
Catalase	Indole production
Cytochrome oxidase	Starch hydrolysis
Voges-Proskauer test	Sucrose, galactose, adonitol, arabinose, cellobiose, inulin, sorbitol, mannose, lactose, melibiose, raffinose, rhamnose, mannitol, maltose
Reduction of nitrate, Gelatinase Casein hydrolysis, D-glucose, fructose, maltose, salicin, trehalose, and xylose	
Electron acceptors, e.g. Fe(III), selenate	Inositol

of inhibitor II compared to inhibitor I. It could be explained that ACE4 utilizes the inhibitors as organic source with inorganic nutrients from the BH media for their proliferation. It indicates that inhibitor II enhanced the proliferation of the ACE4.

Corrosion inhibitor I

FTIR spectrum of corrosion inhibitor I (Fig. 2a) shows N–H stretching bands in the range of 3200–3400 cm^{-1} and the N–H stretching occurs at 2662 cm^{-1}. It is due to the amine group present in the inhibitor I. The unsaturated olefinic band or aromatic =C–H occurs at 3050 cm^{-1}. The aromatic or unsaturated olefinic band is observed in the range of 1800–1750 cm^{-1}. The strong band at 1705 cm^{-1} is due to C=O stretching band, it indicates the presence of carboxylic acid group in inhibitor. The peaks at 1454 and 1279 cm^{-1} are due to C–N asymmetric and symmetric stretching bands. The peak at 933 cm^{-1} is substituted benzene ring band or olefinic out-of-plane bending band. The peak at 734 cm^{-1} is due to aromatic plane bending C–H band for the presence of benzene ring or olefinic out-of-plane bending C–H band.

In the presence of bacteria with corrosion inhibitor I (Fig. 2b), the N–H stretching bands are observed in the range of 3200–3400 cm^{-1} and the unsaturated olefinic band (=C–H) occurs at 3050 cm^{-1}. The methyl (CH_3) and methylene (CH_2) protons are observed in the range of 2922 and 2857 cm^{-1}, respectively. The N–H stretching band occurs at 2677 cm^{-1}. The olefinic (=C–H) overtone band is observed between 1900 and 1950 cm^{-1}. The strong band at 1706 cm^{-1} is due to C=O stretching band. The peaks at 1454 and 1267 cm^{-1} are due to C–N asymmetric and symmetric stretching bands. The peak at 933 cm^{-1} indicates the presence of pi-substituted benzene ring due to the substitution reaction induced by bacteria and a peak at 734 cm^{-1} is due to olefinic or aromatic C–H out-of-plane bending band. FTIR spectrum reveals that the substitution reaction occurs in benzene ring, which is due to the bacterial activity.

NMR spectrum of corrosion inhibitor I shows the characteristic band in Fig. 3a. The multiplet peaks at 7 ppm are due to aromatic C–H protons. The singlet peak at 5.37 ppm is due to olefinic proton. Two types of amine protons can be observed, and one as a quartet in 2.59–2.57 ppm. The amine proton peak is observed from 2.15 to 2.39 ppm. The aliphatic methylene (CH_2) peaks are noticed at 1.1 and 1.2 ppm and the methyl proton peaks are observed at 0.89 and 0.99 ppm. It reveals the presence of olefinic protons and amine-based compounds in corrosion inhibitor I. In the presence of bacteria (Fig. 3b), the two types of olefinic protons can be observed at 5.35, 5.33 and 5.28 ppm. The disappearance of aromatic protons at 7 ppm reveals that bacteria consumed the aromatic compound and formed the olefinic compound via 5.33 and 5.35 ppm as a doublet peak and

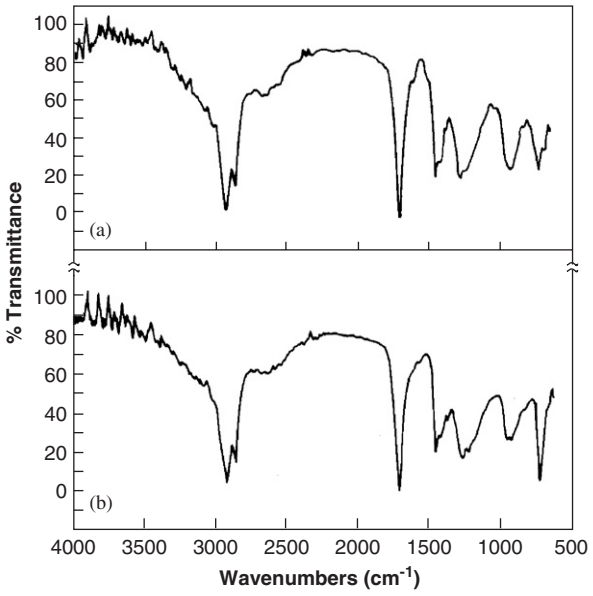

Figure 2. Fourier-transform infrared spectrum. (a) Corrosion inhibitor I (uninoculated system- control). (b) Inoculated with *Bacillus cereus* ACE4.

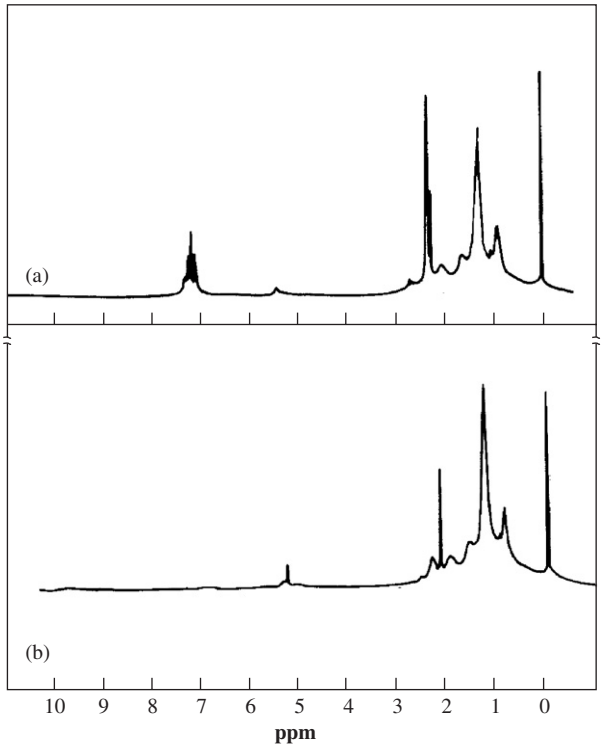

Figure 3. H^1 NMR Spectrum: (a) corrosion inhibitor I (uninoculated system – control) and (b) inoculated with *Bacillus cereus* ACE4.

5.28 ppm singlet peak. The amine proton peak is observed in the range of 1.85–2.51 ppm as a mutiplet peak and aliphatic peak is noticed at 1.58 and methyl protons can be noticed at 0.28 and 0.97.

HPLC spectrum for corrosion inhibitor I is presented in Fig. 4. In control system (uninoculated system), five peaks can be noticed, which indicates the presence of five components in the inhibitor I (Fig. 4a). The peak areas of the five components are ranging between 5.9 and 579.2 mV s. The highest peak (area, 592.5 mV s) alone can be noticed in the presence of ACE4 inoculated system (Fig. 4b). It indicates that bacteria consume all the components within 30 days, except a component at 3.910 retention time; whereas 86% of concentration reduction (61.61 mV s) can be noticed.

Corrosion inhibitor II

FT-IR spectrum of corrosion inhibitor II shows (Fig. 5a) the presence of the N–H stretching bands in the range of 3250–3400 cm^{-1}. It is due to the amine group present in the inhibitor and the aromatic C–H stretching band is observed at 3050 cm^{-1}. The methyl (CH_3) and methylene (CH_2) aliphatic saturated C–H stretching bands are observed at 2922 and 2856 cm^{-1}, respectively. The N–H stretching band can be noticed at 2662 cm^{-1}. The aromatic overtone band or olefinic (=C–H) is observed in the range of 1900–1800 cm^{-1}. The C=O stretching band is observed at 1700; it is due to the presence of carboxylic acid group. The peak at 1554 cm^{-1} is due to aromatic C=C stretching band and the peak at 1456 cm^{-1} is due to aromatic C–C stretching band. The C–N asymmetric stretching is observed at 1397 cm^{-1} and C–N symmetric stretching is observed at 1304 cm^{-1}.

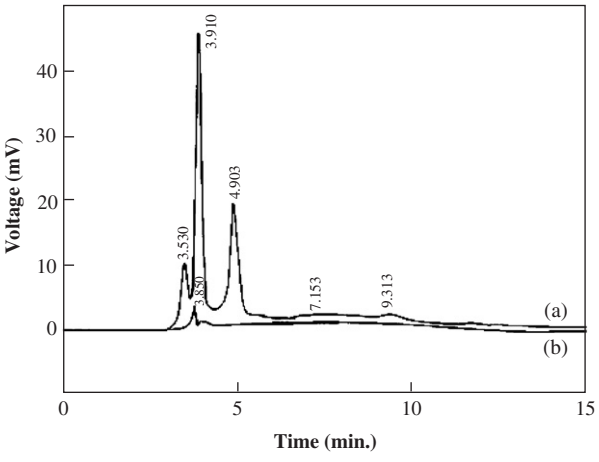

Figure 4. HPLC spectrum for corrosion inhibitor I: (a) Corrosion inhibitor I (uninoculated system – control) and (b) inoculated with *Bacillus cereus* ACE4.

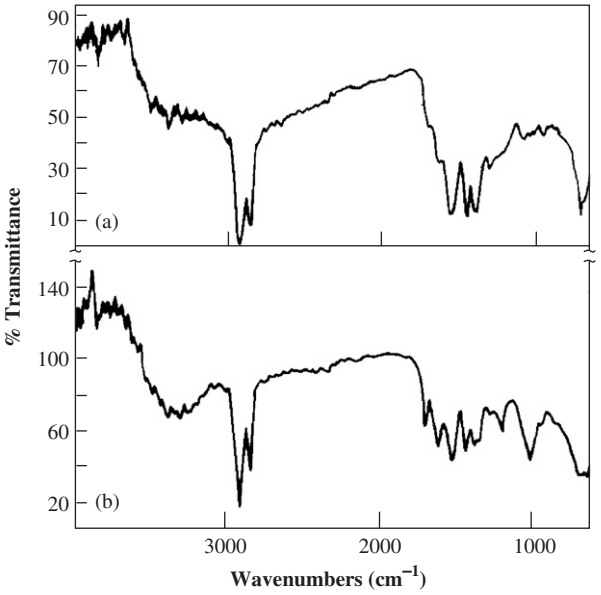

Figure 5. Fourier-transform infrared spectrum: (a) Corrosion inhibitor II (uninoculated system – control) and (b) Inoculated with *Bacillus cereus* ACE4.

The peak at 1078 cm^{-1} is due to aromatic C–O–C delocalization band. The peak at 968 cm^{-1} is due to the substituted benzene ring. The aromatic bending band occurs at 722 cm^{-1}.

In the FT-IR spectrum of corrosion inhibitor II in bacterial inoculated system, (Fig. 5b) the N–H stretching band can be observed in the range of 3250–3500 cm^{-1}. The olefinic (=C–H) stretching band is observed at 3050 cm^{-1}. The aliphatic methyl (CH_3) and methylene (CH_2) C–H stretching bands are observed at 2919 and 2854 cm^{-1}, respectively. The N–H stretching band is observed at 2662 cm^{-1}. The C=O stretching band is observed at 1716 cm^{-1}, whereas the N–H plane-bending band can be observed at 1641 cm^{-1}. The C=C stretching band at 1549 cm^{-1} and C–C stretching band at 1400 cm^{-1} are also observed. The C–N asymmetric band occurs at 1400 cm^{-1} and the symmetric stretching band occurs at 1227 cm^{-1}. The olefinic C–C stretching band can be noticed at 1048 cm^{-1} and olefinic (=C–H) out-of-plane bending band is observed at 730 cm^{-1}. The disappearance of peak at 968 and 722 cm^{-1} (benzene ring out-of-plane bending band) is due to the consumption of aromatic compound by the bacterial activity. The NMR spectrum of corrosion inhibitor II is shown in Fig. 6a. The aromatic proton peak is observed at 7 ppm as a singlet peak. The olefinic (=C–H) proton peak occurs at 5.32 ppm. The amine protons are observed at 3, 2.79 and 2.29–1.9 ppm and the aliphatic methylene (CH_2) protons peak is observed at 1.59 and 1.29 ppm.

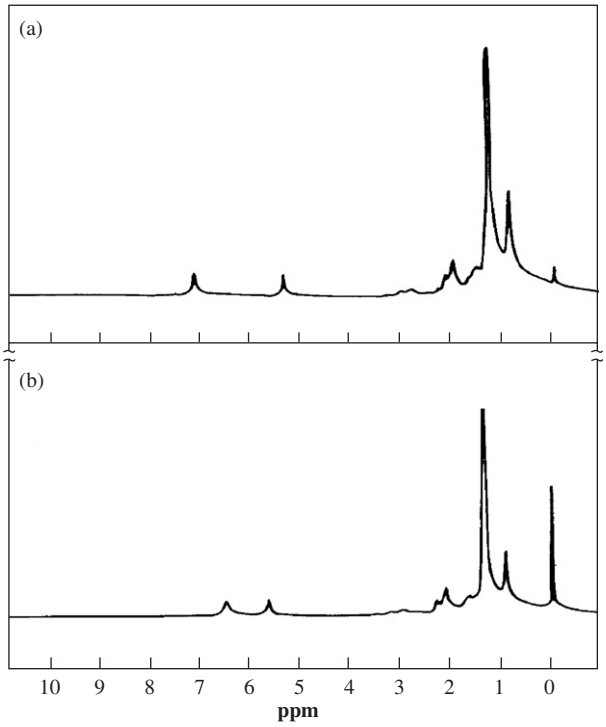

Figure 6. H^1 NMR Spectrum:(a) Corrosion inhibitor II (uninoculated system – control) and (b) Inoculated with *Bacillus cereus* ACE4.

A methyl proton (CH_3) peak can be noticed at 0.87 ppm. In the NMR spectrum of corrosion inhibitor II in bacterial inoculated system (Fig. 6b), two types of olefinic protons are observed. The singlet peak at 6.1 ppm is for olefinic protons; formed from the decomposition of aromatic ring and the olefinic proton peaks can be observed as singlet peak at 5.33 ppm. The amine proton peaks are observed at 2.82 ppm, and ranging between 2.02 and 2.19 ppm. The aliphatic methylene proton peaks are observed at 1.5 and 1.28 ppm and the methyl proton peak is observed at 0.91 ppm.

The GC retention data of the inhibitor II correspond to structural assignations performed after NIST (library search) with a database and by mass spectra interpretation are presented in Table 2. From the GC-MS analysis (Fig. 7), it was observed that the corrosion inhibitor (uninoculated system) consists of aliphatic hydrocarbons, including cyclohexane, octadecyne, n-hexodecanoic acid, nonen, tetradecane, and aromatic carbons, including benzene 1,2-diethyl, pyridine and phenol. The major component is oleic acid. In the presence of ACE4 (Fig. 8), it utilizes the aliphatic components including nonen-2 one, 1-octadecyne, cyclohexane, hexodecanoic acid, propenoic acid and aromatic compounds like benzene, 1,2-diethyl, phenol. The new compounds can be observed at 7.23 retention

Table 2. GC-MS data of pure corrosion inhibitor II

Retention time (min)	Compound
0.90	1-Hexadecanol
1.00	3-Nonen-2 one
1.07	1-Octadecyne,
1.10	Cyclohexane, 1-methyl 2-propyl
1.24	2.propennic acid octyl ether
1.35	Benzene, 1,2,3,5-tetramethyl
1.72′	Tetradecane, 1-chloro
1.55	Benzene, 1,2 diethyl
11.22	N-Hexadecanoic acid
13.16	Oleic acid
13.35	Pyridine, 2-tridecyl
15.14	Pyridine, 2-tridecyl
15.94	Phenol,2,6-di(t-butyl)-4(cyclohexancylidene) amino
14.30	Pyridine, 2-tridecyl

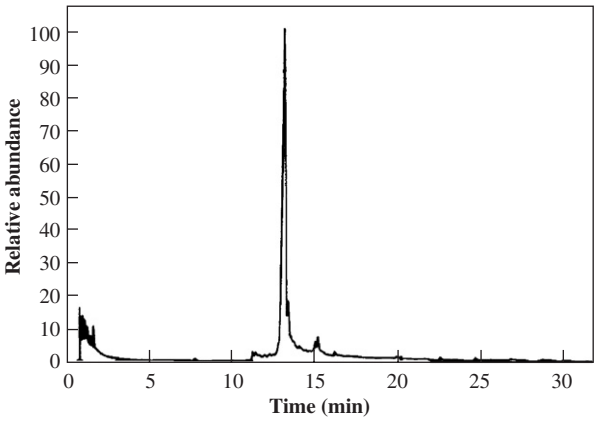

Figure 7. GC-MS spectrum of pure corrosion inhibitor II.

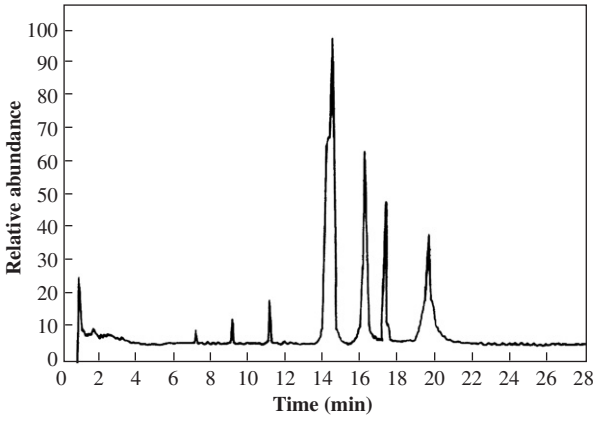

Figure 8. GC-MS spectrum of corrosion inhibitor II inoculated with ACE4.

time which indicates the presence of phenyl 2,4-di-tet-butyl due to the decomposition or degradation of aromatic compounds (Table 3). The finding suggests that the strain ACE4 has the high preference to degrade both aliphatic and aromatic components.

The present study reveals that the isolate has the capacity to degrade both the aromatic and aliphatic hydrocarbon in the corrosion inhibitors I and II in petroleum product pipeline. Videla et al. (2000) also noticed microbial degradation of film-forming inhibitor and observed that *Pseudomonas* sp. isolated from injection water, degraded several aromatic compounds and generated energy for its metabolic activity. They also suggested that dimethylamine, imidazoline, morpholine, cyclo hexylamine and quaternary ammonium compounds are biodegradable.

Table 3. GC-MS data of corrosion inhibitor II after 30 days of inoculation with strain ACE4

Retention time (min)	Compound
Strain ACE4	
0.90	1-Hexadecanol
7.23	Phenyl, 2,4-di-tet-butyl
9.14	Heptacosane
14.32	Oleic acid
17.18	Oleic acid eico ester
19.52	Oleic acid, 9-octacenyl ester

Inhibitor efficiency

Rotating cage test

The inhibition efficiency (IE) of corrosion inhibitors I and II is presented in Table 4. The corrosion rate of API 5 LX in control system (without inoculum) is ranging between 0.04 and 0.07 mm/year up to 240 h. In the presence of microbes and absence of corrosion inhibitor (system-II), the corrosion rate is higher in the range between 0.08 and 0.12 mm/yr than in the absence of microbes. Inhibitor I gives inhibition efficiency ranging between 90% and 93% while inhibitor II gives the efficiency ranging between 56% and 88% up to 240 h in the absence of bacteria. In the presence of inhibitor I along with bacteria, the inhibition efficiency is between 66% and 76%, while adding inhibitor II with bacteria the efficiency reduces and it is ranging between 31% and 40% up to 240 days.

Table 4. Corrosion rates of API 5LX with corrosion inhibitors in different system

S .no.	System	Immersion period (h)	Weight loss (mg)	Corrosion rate (mm/yr)	Inhibition efficiency (%)
1	500 ml diesel+2% water	80	5.75	0.04	—
		160	20.25	0.07	—
		240	29.85	0.07	—
2	500 ml diesel+2% water+ACE4	80	10.36	0.08	—
		160	29.15	0.11	—
		240	49.51	0.12	—
3	500 ml diesel+2% water+corrosion inhibitor I (10 ppm)	80	0.381	0.003	93
		160	2.06	0.008	90
		240	2.61	0.001	91
5	500 ml diesel+2% water+corrosion Inhibitor II (10 ppm)	80	2.53	0.019	56
		160	8.41	0.031	88
		240	12.78	0.031	57
4	500 ml diesel+2% water+ACE4+corrosion inhibitor I (10 ppm)	80	3.49	0.026	66
		160	7.24	0.027	75
		240	11.69	0.029	76
5	500 ml diesel+2% water+corrosion inhibitor II (10 ppm)+ACE4	80	2.53	0.052	31
		160	8.41	0.064	40
		240	12.78	0.075	38

The present observation reveals that bacteria reduces the efficiency of inhibitors I and II about 22% and 35%, respectively.

Surface analysis

The FTIR spectrum of the surface film on the metal surface exposed to corrosion inhibitors I and II with ACE4 is shown in Fig. 9. In the presence of bacteria with corrosion inhibitor I (Fig. 9a), the peak shown is noted in the range of 2954 and 2923 cm^{-1}, which are assigned to the presence of –CH– aliphatic stretching. New peaks are noticed at 1463 and 1378 cm^{-1} and are due to CH def for CH_3 group and a peak at 1020 cm^{-1} indicates the presence of stretching for –C–O–C– group. A peak at 884 cm^{-1} indicates the di-substituted benzene and another peak at 559 cm^{-1} indicates the presence of iron peak. The absence of peaks at 1705 (C═O), 1454 (C═N), 1279 (C–N), 933 and 734 for substituted benzene ring bond are noticed when compared to corrosion inhibitor I (Fig. 2a). In the presence of corrosion inhibitor II with ACE4 (Fig. 9b) the new peaks at 1464, and 1378 cm^{-1} are due to CH def for CH_3 group. The peak at 1021 cm^{-1} indicates the presence of stable –C–O–C– group, and di-substituted benzene at 884. The peak at 534 cm^{-1} indicates the presence of iron peak. Although complex is formed on the metal surface, due to the degradation of inhibitor/diesel at the interface act as humic substance, resulting in the high supply of electron to the metal surface and accelerates the corrosion. It can be inferred that the corrosion inhibitor coordinated with Fe^{2+} through the –C–O–C- and carbonyl oxygen resulting in the formation of Fe^{2+}-corrosion inhibitors complex on the metal surface. The absence of peak at 1554 (C═C), 1456 (–C–C–), 1397 (C–N), 1304 (C–N), 968 and 722 di-substituted benzene is noticed when compared to corrosion inhibitor II (Fig. 5a).

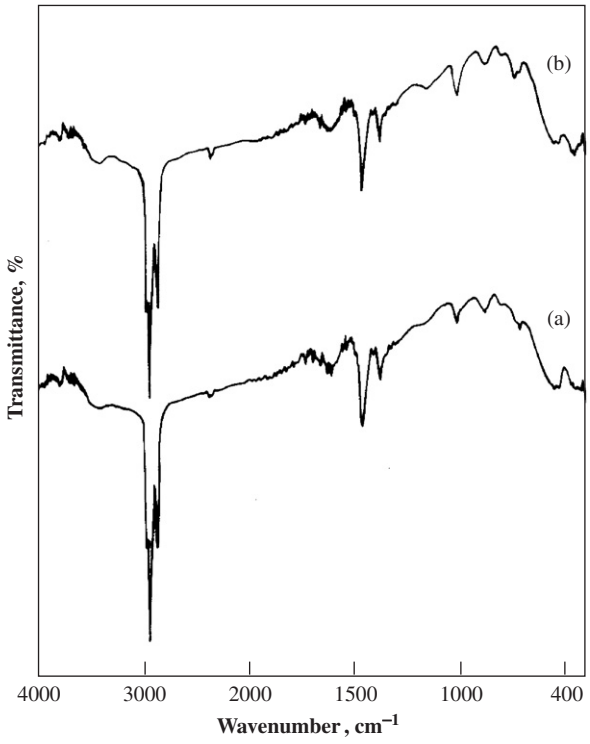

Figure 9. Surface film on the metal surface in the presence of corrosion inhibitors with ACE4: (a) Corrosion inhibitor I with ACE4 and (b) corrosion inhibitor II with ACE4.

Electrochemical study

Figure 10 shows the polarization curve for API 5LX in diesel–water systems in the presence and in the absence of bacterium ACE4 and corrosion inhibitors. The data collected from polarization are presented in Table 5. The corrosion current for control system I (only 120 ppm chloride) is 9.88×10^{-7} A/cm^2 and the b_a value is 980 mV/decade. The anodic curve also shows passivation and it indicates that corrosion is lesser than the other systems. In the presence of bacteria (system II), the corrosion current is 1.81×10^{-6} A/cm^2, while in the presence of corrosion inhibitors I and II, the corrosion currents are 1.87×10^{-6} and 1.88×10^{-5} A/cm^2, respectively. Inhibitor II enhances the corrosion current about one order from the bacterial system (control system II) and two orders from the control system I (only chloride). The b_c value for inhibitor II along with bacteria is

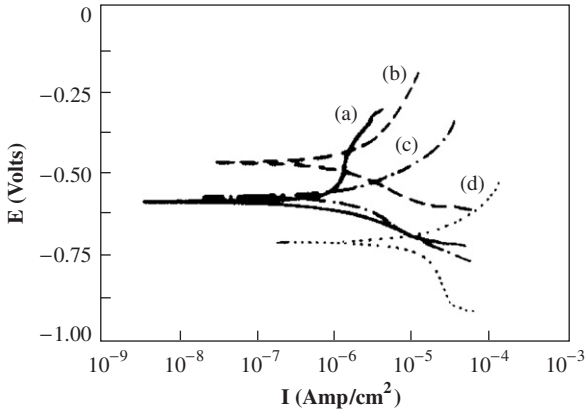

Figure 10. Polarization curves for API 5LX in diesel water system, in the presence/absence of ACE4 for different systems: (a) 500 ml diesel+2% water, (b) 500 ml diesel+2% water+ACE4, (c) 500 ml diesel+2% water+ACE+corrosion inhibitor I (10 ppm) and (d) 500 ml diesel+2% water+ACE+corrosion inhibitor II (10 ppm).

Table 5. Corrosivity of the various systems

Systems	E_{corr} (mV)	b_a (mV/decade)	b_c (mV/decade)	I_{corr} A/cm^2
500 ml diesel+2% water	−579	980	80	9.88×10^{-7}
500 ml diesel+2% water+*B. cereus* ACE4	−457	228	90	1.81×10^{-6}
500 ml diesel+2% water+*B.cereus* ACE4+corrosion inhibitors I	−562	136	142	1.87×10^{-6}
500 ml diesel +2% water+*B.cereus* ACE4+corrosion inhibitors II	−700	167	460	1.88×10^{-5}

Table 6. Impedance parameters for API 5 LX carbon steel in various systems

S. no.	Systems	R_s (faraday)	R_{ct} ($k\Omega$ Cm^2)
1	500 ml diesel+2% water	51 Ω cm^2	9.98
2	500 ml diesel+2% water+*B. cereus* ACE4	163 Ω cm^2	7.67
3	500 ml diesel+2% water+*B. cereus* ACE4+corrosion inhibitors I	3.08 kΩ cm^2	7.58
4	500 ml diesel+2% water+*B. cereus* ACE4+corrosion inhibitors II	0.84 kΩ cm^2	2.06

higher than the other systems. These curves reveal that the corrosivity of the systems inhibitors I and II are higher than of the control. The nature of the curve for API 5LX in the presence of sodium chloride shows slight passivation. In the second system (ACE4 with 1% BH broth), ACE4 increases the cathodic current (cathodic depolarization) and slightly enhances the anodic current when compared to system I. It can be explained that the biodegraded products dissolve in water and supply electron to metal surface, which accelerates the cathodic reduction process. The end products of acid slightly influence the anodic process also. In the presence of inhibitor I, the dissolved amine proton in water may decrease the cathodic current, whereas the anodic current is increased by the metabolic products of the bacteria dissolved in the contaminated water. Besides, it can be concluded that the dissolved products of inhibitor II enhance both the anodic and cathodic reactions. It may be due to the higher degradation of inhibitor II than of inhibitor I.

R_s and R_{ct} values were derived from the impedance measurements and are presented in Table 6 and Fig. 11. The R_s values for control system and bacterial system (sodium chloride) are ranging between 51 and 163 Ω cm^2. In the presence of inhibitors I and II, the R_s values are 3.08 and 0.84 kΩ cm^2, respectively. The R_s value of inhibitor I is higher than of inhibitor II. It may be due to the solubility of degraded components of inhibitor in diesel/water system. The high solution resistance indicates the stability of the product, which may be the reason for the failure in GC-MS analysis. The R_{ct} values for control system is 9.98 kΩ cm^2; which is

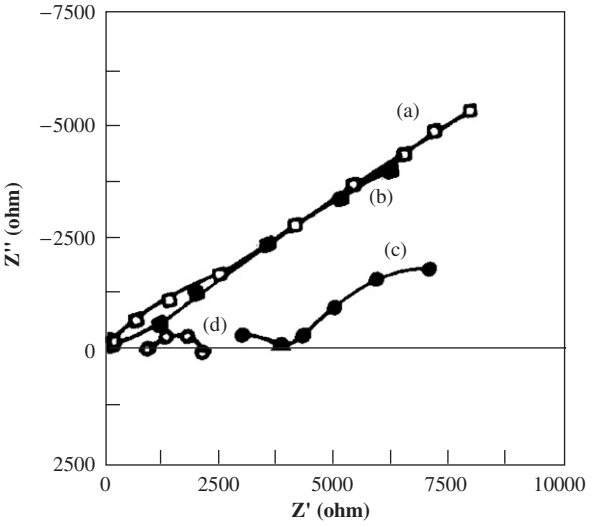

Figure 11. Impedance curves for API 5LX in diesel water system, in the presence/absence of ACE4 for different systems: (a) 500 ml diesel+2% water, (b) 500 ml diesel+2% water+ACE4, (c) 500 ml diesel+2% water+ACE+corrosion inhibitor I (10 ppm) and (d) 500 ml diesel+2% water+ACE+corrosion inhibitor II (10 ppm).

higher than of other systems. It supports the polarization and weight-loss results. In the presence of bacterial system, the resistance is 7.67 kΩ cm^2; while adding inhibitors, the R_{ct} values are ranging between 2.06 and 7.58 kΩ cm^2. The reduction of R_{ct} value of inhibitor II supports the polarization study and it can be explained that due to the degradation of inhibitor, the efficiency decreased. In the presence of chloride system, the nature of the curve (45° slope) reveals that the

diffusion controlled reaction, while in the presence of bacteria, small semicircle along with straight line indicates the presence of adsorbed biofilm, followed by diffusion control reaction. In the presence of inhibitor I, the curve shows two capacitive loops: the first capacitive loop is relatively small when compared to the second. The first capacitive loop is well defined with high frequency range. The low frequency part of the diagram is not clearly defined. The high frequency part represents the formation of intact part of the adsorbed film (Ashassi-Sorkhabi et al., 2002), whereas the low frequency data points are associated with the Faradic process occurring on the bare metal through defects and pores in the adsorbed inhibitor layer. But in the presence of inhibitor II, only activation control (anodic reaction) can be noticed. It reveals that the degraded product of inhibitor I adsorbs on the metal surface and influences the electrochemical behavior of metal. Hence, the selection of good non-biodegradable inhibitor or good biocide is an important criterion for petroleum product pipelines.

Generally, bacteria utilize energy from the environment by consumption of carbon and phosphorous in the ratio 40:1; if these consume excess, these release out in the form of glucose-6-phosphate and fructose-6-phosphate (Malony et al., 1990). In the present study, bacterium was inoculated in inhibitor degradation and corrosion inhibition studies along with BH broth. In the present study, 1% of BH broth was added in corrosion inhibition and degradation study, respectively, because inorganic nutrients are also needed for bacterial physiological activity. Since organic and inorganic nutrient sources are needed for bacterial physiology, BH broth was added with bacteria for corrosion evaluation study. Though 1% BH broth consists of 10 ppm phosphate and 10 ppm nitrate, the effect of nutrient on the metal surface should also be considered as an important factor. Cohlen (1976) suggested that phosphates can influence the anodic reaction in aerated solution, whereas the phosphate film was formed by reaction with dissolved oxygen. Because the ferrous phosphate has some solubility in water, the corrosion reaction is not totally eliminated but is rather reduced to manageable degree (Pryor and Cohen, 1953). Franklin et al. (1990, 2000) investigated the effect of biofilm on mild steel surface in the presence of phosphate and other anions (chloride and sulfate). They found that bacterial biofilm enhanced the propagation of pits, probably because of the uptake of phosphate by the microorganisms. Bento et al. (2004) concluded that the dissolved oxygen has an important role in the phosphate-induced passivity of mild steel in the presence of filamentous fungi, *Hormoconis resinae*, *Paecilomyces variotii*, *Aspergillus fumigatus*, the bacterium *Bacillus subtilis* and the yeast *Candida silvicola*. The anodic and cathodic potentiostatic polarization curves after 30 and 60 days of incubation showed regions corresponding to active dissolution, although the condition in the sterile medium used in the experiments favored passivation of the metal. The film in the presence of chloride ion in Bushnell Hass medium showed a quite different beaviour. No passivation region was observed in polarization curves and the high anodic currents registered were associated with the dissolution of iron. But in the present study, in the presence of 120 ppm chloride without BH broth, passivation was noticed. It indicates that the impact of bacterial physiology on metal surface is lesser when compared to the other systems. The higher corrosion rate in the presence of BH broth with ACE4 may be due to the adsorption of both inorganic nutrients with ACE4. Since bacteria cannot be separated from nutrients, the physiological activity of bacteria accelerates the corrosion rate in the presence of organic inhibitor. In the present study, due to the presence of organic and inorganic nutrients, bacteria may degrade both inhibitor and diesel for energy purpose and the degraded products of inhibitor/diesel on metal surface determine the electrochemical behavior of API 5 LX. The present investigators feel that the nature of the polarization may also depend on the degraded products in water and the role of microbes on carbon steel. Hence, the degradation should be avoided by employing non- degradable corrosion inhibitor to control corrosion.

Conclusions

The performance of an organic film-forming corrosion inhibitor was assesse towards its corrosion inhibitive efficiency in controlling the corrosion of API 5LX steel in petroleum product containing bacterial contaminant *B.cereus* ACE4. The dominating isolate *Bacillus cereus* ACE4 (AY912105) was identified in petroleum product pipeline by 16S DNA. This isolate has the capacity to degrade the aromatic and aliphatic carbon present in the corrosion inhibitor. It reduces the corrosion inhibition efficiency of inhibitor by about 35%. The present study reveals that non-degradable corrosion inhibitor is needed for petroleum product pipeline to avoid the microbial degradation of corrosion inhibitors.

Acknowledgments

The authors thank N. Muthukumar for his help in taking Fourier transform infrared spectroscopy (FTIR) and nuclear magnetic resonance spectroscopy (NMR) and related discussions. Dr. K. Pitchumani and Mr. Vijayakumar of the School of Chemistry, Madurai Kamaraj University for their help in GC-MS analysis. The authors are grateful to S. Mohanan, P. Subramanian and S. Ponmariappan for their help in field collection at petroleum product pipeline, North West India.

References

Ashassi-Sorkhabi, H., Nabavi-Amri, A.S., 2002. Polarization and impedance methods in corrosion inhibition study of carbon steel by amines in petroleum-water mixtures. Electrochimica Acta. 47, 2239–2244.

Ausubel, F.M., Brent, R., Kingston, R.E., Moore, D.D., Seidelman, J.G., Struhl, K.E., 1988. Current Protocols in Molecular Biology. Wiley, New York.

Altschul, S.F., Warren, G., Miller, W., Myers, E.W., Lipman, D.J., 1990. Basic local alignment search tool. J. Mol. Biol. 215, 403–410.

Bento, F.M., Gaylarde, C.C., 2001. Biodetrioration of stored diesel oil: studies in Brazil. Int. Biodeterior. Biodeg. 47, 107–112.

Bento, F.M., Englert, G.E., Gaylarde, C.C., Muller, I.L., 2004. Influence of aqueous phase on electrochemical biocorrosion tests in diesel/water systems. Mater. Corrosion 55 (8).

Bento, F.M., Beech, I.B., Gaylarde, C.C., Englert, G.E., Muller, I.L., 2005. Degradation and corrosive activities of fungi in a diesel–mild steel–aqueous system. World J. Microbiol. Biotechnol. 21, 135–142.

Burger, E.D., 1998. Method for inhibiting microbiologically influenced corrosion. US Patent 5,753,180.

Cohlen, M., 1976. The breakdown and repair of inhibitive films in neutral solution. Corrosion 32 (12), 461–465.

Holt, J.G., Kreig, N.R., Sneath, P.H.A., Stanely, J.T., 1994. In: Williams, S.T. (Ed.), Bergey's Manual of Determinative Bacteriology. Williams and Wilkins Publishers, Maryland.

Franklin, M.J., White, D.C., Isaacs, H.S., 1990. International Congress on Microbially Influences Corrosion and Biodeterioration, Tennessee, USA, vol. 3, pp. 35–41.

Franklin, M.J., White, D.C., Little, B., Ray, R., Pope, R., 2000. Spatial and temporal relationships between localized corrosion and bacterial activity on iron-containing substrata. Biofouling 15, 13–23.

Freiter, E.R., 1992. Effect of a corrosion inhibitor on bacteria and microbiologically influenced corrosion. Corrosion 48 (4), 266–276.

Graves, J.W., Sullivan, E.H., 1996. Internal corrosion in gas gathering system and transmission lines. Mater. Prot. 5, 33–37.

Hamilton, W.A., 1985. Sulphate-reducing bacteria and anaerobic corrosion. Annu. Rev. Microbiol. 39, 195–217.

Jana, J., Jain, A.K., Sahota, S.K., Dhawan, H.C., 1999. Failure analysis of oil pipelines. Bull. Electrochem. 15, 262–265.

Jan-Roblero, J., Romero, J.M., Amaya, M., Le Borgne, S., 2004. Phylogenetic characterization of a corrosive consortium isolated from a sour gas pipeline. Appl. Microbiol. Biotehnol. 64, 862–867.

Jones, D.A., Amy, P.S., 2002. A thermodynamic interpretation of microbiologically influenced corrosion. Corrosion 58, 638–645.

Little, B., Ray, R., 2002. A perspective on corrosion inhibition by biofilms. Corrosion 58, 424–428.

Malony, P.C, Ambudkar, S.V, Anantharam, V., Sonna, L.V., Veradhachamy, A., 1990. Microbail. Rev. 54, 1–17.

Maruthamuthu, S., Mohanan, S., Rajasekar, A., Muthukumar, N., Ponmarippan, P., Subramanian, P., Palaniswamy, N., 2005. Role of corrosion inhibitor on bacterial corrosion in petroleum product pipelines Ind. J. Chem. Tech. 12 (5), 567–575.

Muthukumar, N., Mohanan, S., Maruthamuthu, S., Subramanian, P., Palaniswamy, N., Raghavan, M., 2003. Role of *Brucella* sp. and *Gallionella* sp. in oil degradation and corrosion. Electrochem. Comm. 5, 421–427.

Papavinasam, S., Review, R.W., Attard, M., Demoz, A., Sun, H., Donini, J.C., Michaelian, K.H., 2000. Laboratory methodologies for corrosion inhibitor selection. Mater. Perform. 39 (8), 58.

Poupin, P., Truffaut, N., Combourieu, B., Besse, P., Sancelme, M., Veschambre, H., Delort, A.M., 1998. Appl. Environ. Microbiol. 64 (1), 159.

Pope, D.H., Pope, R.M., 1998. Guide for the monitoring and treatment of microbiologically induced corrosion in the natural gas industry. GRI report GRI-96/0488. Gas Research Institute, Des PlainesIll.

Prasad, R., 1998. Selection of Corrosion Inhibitors to Control Microbiologically Influenced Corrosion, CORROSION/98, paper no. 276, NACE International, Houston, TX.

Pryor, M.J., Cohen, M., 1953. The inhibition of the corrosion inhibitor of iron by some anodic inhibitors. J. Electrochem. Soc. 100 (1), 203–215.

Rajasekar, A., Maruthamuthu, S., Muthukumar, N., Mohanan, S., Subramanian, P., Palaniswamy, N., 2005. Bacterial degradation of naphtha and its influence on corrosion. Corro. Sci. 47, 257–271.

de Schiapparelli, E.R., de Meybaum, B.R., 1980. Microbial contamination and corrosion of aircraft integral fuel storage tanks. Eval. Risk Control Mater. Perform. 19 (10), 47.

Romero Dominguez, J.R., Garcia Caloca, G., Mendoza Flores, J., lbarra Nunez, E.M., 1998. Study on the Presence of *Pseudomonas fluorescens* on the Efficacy of Three Corrosion Inhibitors (in Spanish), 3rd NACE Latin American Region Corrosion Congress, Cancun, Q.Roo, Mexico, Book of abstracts, pp. 51–52.

Shennan, J.L., 1988. Control of microbial contamination of fuels in storage. In: Houghton, D.R., Smith, R.N.,

Eggins, H.O.W. (Eds.), Biodeterioration. Elsevier, Barking, pp. 248–254.
Videla, H.A., Characklis, W.G., 1992. Biofouling and microbially influenced corrosion. Int. Biodeterior. Biodeg. 29, 195–212.
Videla, H.A., Gdmez de Saravia, S.G., Guiamet, P.S., Allegreti, P., Furlong, J., 2000. Microbial degradation of film-forming inhibitors and its possible effects on Corrosion inhibition performance corrosion/2000, paper no.00386 (Houston, TX, NACE International, 2000).
Von Wolzogen Kuhr, C.A.H., Vander Klugt Water, I.S., 1934. The graphitization of cat iron as an electrochemical process in anaerobic solid. Water 18, 147–165.
Voordouw, G., Shen, Y., Harrington, C.S., Telang, A.J., Jack, T.R., Westlake, D.W.S., 1994. Quantitative reverse sample genome probing of microbial communities and its application to oil field production waters. Appl. Envir. Microbiol. 60, 760c.
Weisburg, W.G., Barns, S.M., Pelletier, D.A., Lane, D.J., 1991. 16S ribosomal DNA for phylogenetic study. J. Bacteriol. 173, 697–703.
Zhu, X.Y., Lubeck, J., Kilbane, J.J., 2003. Characterization of microbial communities in gas industry pipelines. Appl. Environ. Microbiol. 69, 5354–5363.